

Chandra Discovers a Very High Density X-ray Plasma on the O-Star ζ Orionis

Wayne L. Waldron¹ & Joseph P. Cassinelli²

ABSTRACT

We report on a Chandra line spectrum observation of the O supergiant, ζ Orionis (O9.7 Ib). A 73.4 ks HETGS observation shows a wide range of ionization stages and line strengths over the wavelength range of 5 to 26 Å. The observed emission lines indicate a range in temperature of 2 to 10 MK which is consistent with earlier X-ray observations of ζ Ori. Many lines are spectrally resolved showing Doppler broadening of 900 ± 200 km s⁻¹. The observed He-like ions (O VII, Ne IX, Mg XI, and Si XIII) provide information about the spatial distribution of the X-ray emission. Although the observations support a wind distribution of X-ray sources, we find three conflicting results. First, line diagnostics for Si XIII indicate that this line emission forms very close to the stellar surface, where the density is of order 10^{12} cm⁻³, but the velocity there is too small to produce the shock jump required for the observed ionization level. Second, the strong X-ray line profiles are symmetric and do not show any evidence of Doppler blue-shifted line centroids which are expected to accompany an outwardly moving source in a high density wind. Third, the observed velocity dispersions do not appear to correlate with the associated X-ray source radii velocities, contrary to expectations of wind distributed source models. A composite source model involving wind shocks and some magnetic confinement of turbulent hot plasma in a highly non-symmetric wind, appears to be needed to explain the line diagnostic anomalies.

Subject headings: X-rays: stars – Line: profiles– stars: early-type– stars: individual (ζ Ori)– stars: magnetic fields– stars: mass-loss

1. Introduction

The Orion Belt supergiant ζ Ori (O9.7 Ib) is one of the most thoroughly studied hot stars. It has been previously observed in X-rays with the Einstein, ROSAT, and ASCA satellites. Observations with the Einstein Solid State Spectrometer (SSS) found it to be the first O-star to show line emission at Si XIII and S XV (Cassinelli & Swank 1983). ASCA observations show that ζ Ori may have a weak high temperature component greater than 10 MK (Waldron, Corcoran, & Kitamoto 1997), but the majority of the X-ray emission is soft, peaking below 1 keV. The observed X-ray

emission is consistent with the standard O-star relation: $L_X \sim 10^{-7} L_{Bol}$ (Berghöfer et al. 1997), and has remained relatively stable except for a short term of $\sim 15\%$ variability observed during a ROSAT monitoring study by Berghöfer & Schmitt (1994).

It is generally believed that the hot star X-ray emission arises from shocks that develop in the outflowing stellar wind owing to instabilities associated with the line driven wind mechanism (Lucy & White 1980; Owocki, Castor, & Rybicki 1988; Feldmeier 1995). The original X-ray models for hot stars proposed that the X-rays arise from a thin coronal structure located at the base of the stellar wind (Cassinelli & Olson 1979; Waldron 1984). However, the base coronal model was considered inappropriate because early observations did not show significant attenuation of soft X-rays at the oxygen K-shell edge which was expected due

¹Emergent Information Technologies, Inc., Space Sciences Division, 9315 Largo Drive West, Suite 250, Largo, MD 20774; wayne.waldron@emergent-IT.com

²Astronomy Department, University of Wisconsin, 475 N. Charter St., Madison, WI 53706; cassinelli@astro.wisc.edu

to the overlying high density cool wind (Cassinelli & Swank 1983).

The X-ray emission lines produced by a stellar wind distribution of outwardly propagating shocks should show broad profiles with a shape that depends on the wind optical depth (MacFarlane et al. 1991). For an optically thin wind, the predicted profiles are flat-topped and symmetric, whereas, for an optically thick wind, the profile becomes asymmetric, showing a blue-shifted, roughly triangular-shape, owing to the larger attenuation of the line X-rays from the far side of the stellar envelope. The net degree of asymmetry is determined by the number of shocks and the column density, N_w , of the overlying stellar wind. The blue-ward extent of the line reflects the largest outward velocities of the shock fronts.

The Chandra spectrometers have the necessary spectral resolution and sensitivity to test these shock model predictions. In this Letter we present a preliminary analysis of the spectral lines from our Chandra High-Energy Transmission Grating Spectrometer (HETGS) observation of ζ Ori.

2. Observations and Analysis

Our Chandra HETGS observation of ζ Ori was performed in two parts: on 2000 April 8 (04^h08^m - 21^h37^m UT), and on 2000 April 9 (20^h38^m - 01^h05^m UT), with effective exposure times of 59.7 ks and 13.7 ks respectively. ζ Ori is the primary star of a widely separated binary system with an early B-star giant companion, and with Chandra the two components are cleanly separated. Here we use the standard pipeline processed data from our combined 73.4 ks observation to discuss the X-ray line spectrum of ζ Ori A. The high-energy grating (HEG) and the medium-energy grating (MEG) spectra are shown in Figure 1. The range of ions identified indicate an X-ray temperature range of ~ 2 to 10 MK. The triads of He-like lines, commonly known as the “*fir* lines” (see Sec 2.1), of O VII, Ne IX Mg XI and Si XIII are identified in Figure 1.

In this Letter, we focus on the two most obvious features observed in the HETGS spectrum of ζ Ori; (1) the unusual line emission properties of He-like ions, and; (2) the unexpected combination of large line widths and negligible line centroid shifts.

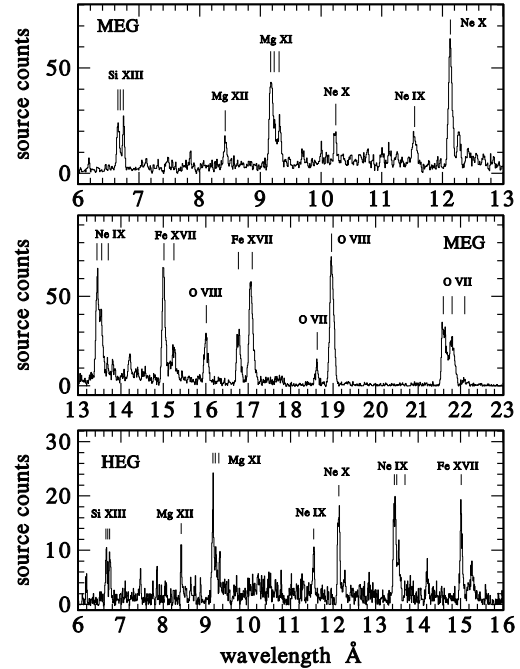


Fig. 1.— Co-added 1st order, background subtracted, Chandra HETGS MEG (top panels) and HEG (bottom panel) count spectra of ζ Ori. The ions responsible for the strongest line emissions are identified. The bin size is 0.01 Å.

2.1. Analysis of He-like Spectral Line Transitions

Gabriel & Jordan (1969) were the first to demonstrate that the *fir* (forbidden, intercombination, and resonance) emission lines of He-like ions can provide very useful diagnostics for the study of X-ray emitting plasmas. They found that the line flux ratio $\mathcal{R} = f/i$ is density sensitive, and the ratio $\mathcal{G} = (f + i)/r$ is temperature sensitive. Although these *fir* line diagnostics have been used extensively in solar studies to derive X-ray electron densities (n_e) and temperatures (T_e) (e.g., Wolfson et al. 1983), the application to O-star spectra requires special care. Blumenthal, Drake, & Tucker (1972), showed that the presence of an external strong UV radiation field can lead to overestimates of the density, since not only collisions, but radiative excitations as well can lead to a decrease in the strength of the *f* line relative to the *i* line. Hence, for O-stars, the observed \mathcal{R} values for several He-like ions, may no longer lead

to a direct measure of n_e , but instead provides information on the radial distance of the X-ray source from the star.

Using the formalism developed by Blumenthal et al. (1972), we calculate the radial dependence of \mathcal{R} in the envelope of ζ Ori using a photospheric UV flux model at $T_{eff} = 30,000\text{K}$ (Kurucz 1993). The radial dependent wind density is derived from the stellar and wind parameters of Lamers & Leitherer (1993) using a standard wind velocity law that is modified below 1.02 stellar radii to provide a smooth density transition to the photospheric structure. The radial dependence of the UV mean intensity $J_\nu(r)$ is assumed to be geometric dilution of the stellar radiation, with no attenuation, i.e., $J_\nu(r) = 4 W(r) H_\nu(T_{eff})$, where $W(r) = \frac{1}{2} \left(1 - \sqrt{1 - (R_*/r)^2} \right)$, and H_ν is given by Kurucz (1993). The predicted \mathcal{R} dependencies for O VII, Ne IX, Mg XI, and Si XIII are shown in Figure 2.

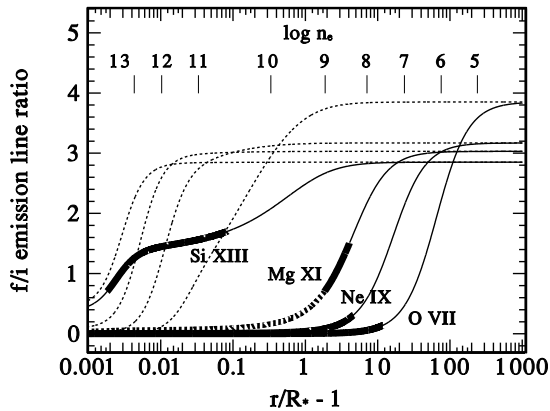


Fig. 2.— The O VII, Ne IX, Mg XI, and Si XIII f/i ratio dependence on geometric dilution (radius) of the UV radiation field and electron density (vertical lines) for the circumstellar environment of ζ Ori. The solid lines include the effects of a UV radiation field (appropriate for hot stars), whereas the dashed lines neglect these effects. The range in the observed f/i ratios are indicated by heavy solid lines. The heavy dashed line for Mg XI is an extension owing to possible overestimates of the f line strength because of contamination from a Mg X line. The corresponding wind densities associated with the radius scale are shown at the top of the panel.

For comparison, we also show the \mathcal{R} dependence for the collision only case, appropriate for very low UV flux.

We find that the predicted \mathcal{R} ratios for the Chandra observed He-like ions, except Si XIII, are controlled by the strength of the UV radiation field, independent of density, as indicated in Figure 2 by the large differences between the collisional and radiative curves. However, for Si XIII the predicted \mathcal{R} ratio shows three regions of dominance, collisional ($n_e > 10^{13} \text{ cm}^{-3}$), constant geometric dilution ($< 1.1R_*$), and a decreasing geometric dilution for large radii. This different \mathcal{R} dependence for Si XIII, as compared to the other three He-like ions, is related to the different strengths of the UV radiation field on the two sides of the Lyman jump. In the case of Si XIII the photo-excitation between the upper levels of the f and i lines ($2^3S \rightarrow 2^3P$) is produced by radiation shortward of 912 Å, where the emergent stellar flux is ~ 8 times smaller than that longward of 912 Å. Figure 2 shows that Si XIII marginally allows for a direct estimate of n_e . Since the other He-like ions have their excitation transition longward of 912 Å, the observed \mathcal{R} ratio can only lead to a measure of the geometrical dilution factor (or radius).

Figure 2 shows the measured range of \mathcal{R} values (given as the heavy solid lines) as a function of radius. The \mathcal{R} values for O VII and Ne IX are extracted from the MEG spectrum, whereas, for Mg XI and Si XIII, the HEG spectrum is used. From Figure 2 we can read off the radii of the X-ray emission line regions, and the associated model dependent electron densities. The most interesting result is the observed \mathcal{R} ratio for Si XIII of 1.2 ± 0.5 which indicates that this line emission originates from the base of the wind, where the electron density is of order 10^{12} to 10^{13} cm^{-3} . The Mg XI \mathcal{R} ratio gives a range in the formation radius of 3 to 5 R_* , and n_e of order 10^9 cm^{-3} . The heavy dashed line for Mg XI in Figure 2 represents the possibility that the f line may be contaminated by a Mg X line since the HEG Mg XI f line shows evidence of a red-shift of $\sim 0.015 \text{ Å}$. The other two ions, O VII and Ne IX, have very weak f emission lines, hence, their \mathcal{R} ratios can only provide upper limits on the source radii of 12 and 6 R_* , corresponding to lower limits on n_e of $4 \times 10^7 \text{ cm}^{-3}$, and $2 \times 10^8 \text{ cm}^{-3}$ respectively. The X-ray location

from Mg XI and upper limits from O VII and Ne IX shown in Figure 2 suggest that some of the X-rays are produced high in the wind, consistent with stellar wind shock predictions (Feldmeier, Puls, & Pauldrach 1997). Furthermore, shocks may still be generated above these upper limits, but they cannot be the dominant source of the He-like X-ray emission lines, otherwise their f line fluxes and \mathcal{R} ratios would be larger than observed.

The X-ray source radii predicted from the f/i analysis (Fig. 2) suggest a systematic ordering of the He-like ions, i.e., high energy ions at low radii and low energy ions at large radii. In a shock picture, a reverse ordering would have been expected, since the shock jump temperature should be proportional to the local wind velocity. This particular anomaly might be explainable by considering the radial distance from which the line emission can be seen by an external observer. Using the wind absorption cross sections of Waldron et al. (1998), we find that the optical depth in the continuum adjacent to a line reaches unity at radii of 1.03, 1.5, 2.8, and 2.2 for Si XIII, Mg XI, Ne IX, and O VII, respectively. These radii are all just less than or equal to the radii predicted by our f/i ratio analysis. We suggest, therefore, that our Chandra observations imply that the X-rays emission lines originate primarily from just above their associated monochromatic X-ray "photosphere" where the continuum radial optical depth is unity.

Finally, using the results of Pradhan & Shull (1981), Wolfson et al. (1983), and Keenan et al. (1994), we extract T_e from the measured \mathcal{G} ratios. For O VII and Ne IX, we find upper limits of 2 and 6 MK, and for Mg XI and Si XIII, ranges of 2 - 11 and 1 - 9 MK are indicated. These temperatures are consistent with the overall observed ion distribution illustrated in Figure 1.

2.2. Analysis of the Emission Line Profiles

After correcting for instrumental broadening, all X-ray lines in ζ Ori are seen to be very broad, with velocity dispersions in the range 900 ± 200 km s⁻¹. Our HETGS observations of ζ Ori show no evidence of any large Doppler blue-shifted asymmetric X-ray line profiles. We also find no indication that the Gaussian width correlates with the ion properties, which suggests that the lines form in the same region or at least in regions

with similar velocity spreads. From the strongest HEG lines, we find a distribution in shifts from line center of ± 0.005 Å which is consistent with the wavelength uncertainty of the HETGS/HEG (Marshall 2000). There are a few MEG spectral lines showing blue-shifts of ~ 0.01 Å (e.g., O VIII, 18.97 Å), but we also see similar red-shifts. In this preliminary analysis we find that there is no observed preference for a systematic blue or red-shift.

Our f/i analysis in Sec. 2.1 indicates a distribution of X-ray sources from ~ 1 to $12 R_*$. However, our observed line profiles appear to show very similar line-width and line-symmetry properties, which seems inconsistent with their being formed over such a large range in radius. To better understand this problem, we explore two distributed shock models. We only focus on those X-ray lines that form above $\sim 1.5 R_*$ which arise from shocks in the wind (i.e., Mg XI, Ne IX, and O VII).

Expanding on the single shock model of MacFarlane et al. (1991), we developed a shock model consisting of 10 spherically symmetric shocks equally distributed between 0.4 to $0.97 v_\infty$, with temperatures ranging from 2 to 10 MK. The shock strength scales with the local wind emission measure, and the wind absorption cross sections are from Waldron et al. (1998). This choice of parameters generates an X-ray source distribution with radius that is consistent with our f/i analysis. The model predictions are shown in Figure 3a for the two limiting cases, optically thick (maximum N_w), and optically thin ($N_w = 0$). In the optically thick case (appropriate for a high density hot star wind), the wind attenuation reduces the contribution to the line emission from the far side of the star and the resultant line emission tends to arise from the highest density regions that are blue-shifted and moving towards us. For the optically thin case, the line emission is narrow and almost symmetric (with a slight asymmetry due to stellar occultation effects). The narrowness arises because emission is proportional to n_e^2 , thus the strongest line emission occurs from regions of low velocity. Comparison of the shock model predictions (Fig. 3a), folded through the MEG instrumental response, with a typical single ζ Ori X-ray line profile (Ne x, 12.13 Å) is shown in Figure 3b, along with the best-fit Gaussian model ($\Delta\lambda_D = 0.042 \pm 0.003$ Å). Clearly the optical thick

line model does not explain the observed line profile, and the optically thin case provides a good fit to the observed symmetry and broadness. However, the optically thin model requires extreme conditions.

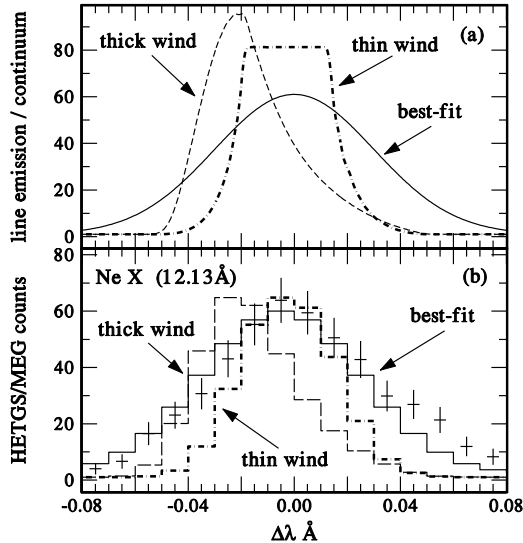


Fig. 3.— X-ray line profile dependence on wavelength shift ($\Delta\lambda$) from line center showing 3 input line profiles and their expected HETGS/MEG count spectra. (a) Model line profiles for a distribution of shocks for an optically thick (dashed line) and thin wind (dot-dashed line). The best-fit Gaussian model profile (solid line) is shown for comparison which required a physical velocity dispersion of $1040 \pm 75 \text{ km s}^{-1}$. (b) Comparison of the observed Ne X line at 12.13 \AA (1 sigma error bars) with model line profiles folded through the instrumental response of the HETGS/MEG.

The wind could be made thin by increasing the ionization structure, which reduces the opacity (Waldron 1984; MacFarlane, Cohen, & Wang 1994). However, for normal hot stars, the winds cannot be uniformly highly ionized because these stars show strong P-Cygni UV line profiles from low ion stages such as C IV, which are distributed throughout the wind (Lamers & Morton 1976). An optically thin wind can also be produced by reducing the mass loss rate, \dot{M} since N_w is proportional to \dot{M} . For example, to maintain an X-ray

line symmetry comparable to the optically thin case shown in Figure 3a, while constraining the sources to lie within $12 R_*$, \dot{M} must be reduced by at least an order of magnitude. However, such a reduction in \dot{M} would be inconsistent with wind line profile analyses (Lamers & Morton 1976) and free-free continuum observations (Lamers, Waters, & Wesselius 1984; Abbott et al. 1980). There are other alternatives. For example, a wind with a clumpy or non-symmetric structure, has been shown to effectively produce an optically thin wind even in stars with relatively large \dot{M} (Moffatt & Robert 1994). In addition, if the shocks are produced at very large stellar radii where the corresponding column densities between equal red and blue-shifted velocities components are negligible, a symmetric line profile can be produced (Feldmeier, private communication). However, to achieve a difference of no more than 10% between the red and blue-shifted velocity components for the Ne X line shown in Figure 3b, we find that the shock would have to be located at $\sim 25 R_*$ which is ~ 2 times larger than the largest formation radius inferred from our f/i analysis.

3. Discussion

Our HETGS observation of ζ Ori has presented several unexpected results. Although the analysis of the He-like ions suggest a stellar wind distribution of X-rays, consistent with a shock model, we also find convincing evidence for X-ray emission from near the stellar surface. Such a source location presents a problem because the wind velocity would be too small to produce a shock jump capable of producing the Si XIII ion stage. The observed X-ray line profiles are very broad and symmetric, and they show no evidence for Doppler blue-shifted line centroids. Since the observations indicate that the shocks must be located within $12 R_*$, the observed line profiles imply that a significant reduction in N_w or \dot{M} is required to explain the observed line symmetry. Even if we can explain the line symmetry problem by applying non-symmetric or clumpy wind structure arguments, we still need an alternative model to explain the origin of the high density, near-surface X-ray plasma from ζ Ori. We suggest that there is magnetic loop confinement as was originally proposed by Cassinelli & Swank (1983) to explain their SSS observations of ζ Ori.

The observed ζ Ori surface X-ray plasma density is about 2 orders of magnitude larger than normal for a quiescent solar magnetic loop (e.g., Vaiana & Rosner 1978), but is comparable to solar flare densities (Phillips et al. 1996). A surface distribution of magnetic loop structures could provide a mechanism for producing a collection of symmetric blue and red-shifted bulk plasma motion, and since both components are near the surface of the star, their emitted X-rays must pass through similar amounts of absorbing material, producing symmetric line profiles like those observed in ζ Ori. Although the observed velocity dispersions are high, they are comparable to predicted solar flare velocity dispersions of order 1000 km s^{-1} (Antonucci, Benna, & Somov 1996). If the high density plasma of ζ Ori is residing in a collection of surface magnetic loops, we can estimate the required magnetic field by assuming a balance between the magnetic and gas pressures (i.e., the plasma β is unity). Using an n_e of 10^{12} cm^{-3} and a T_e of 5 MK leads to a magnetic field strength > 180 Gauss. This is comparable to the field of ~ 200 Gauss detected on the B1 giant β Cephei (Henrichs et al. 2000). The likelihood of such fields on hot stars has been investigated by Cassinelli & MacGregor (1999) who found that fields in hot main sequence stars generated by dynamo action at the interface between the radiative core and convective envelope could rise to the surface. Thus a magnetically confined plasma on the surface of a hot star is certainly plausible.

Because of the n_e^2 dependence of recombination that leads to the He-like ions, the *fir* diagnostic of density or of source location tend to yield values for the densest region producing the lines. This was discussed for the density dominated case by Brown et al. (1991). We find evidence that X-rays are being produced both at dense regions very near the star, and from regions distributed throughout the wind. However, the observed X-ray *line profiles* seem incompatible with their being distributed as shocks throughout the optically thick wind. A more fundamental question that we raise is - why are the velocity dispersions essentially the same regardless of the X-ray source location? Our results provide both new facts and new challenges for future studies of hot star X-ray emission.

We are grateful to Mike Corcoran, Andy Endal, Joe MacFarlane, and Nathan Miller for their useful comments and suggestions. We would also like to thank John Brown for several enlightening conversations, and the referee, Achim Feldmeier, for his detailed critique of our manuscript, and several informative suggestions.

REFERENCES

- Abbott, D. C., Biegging, J. H., Churchwell, E., & Cassinelli, J. P. 1980, *ApJ*, 238, 196
- Antonucci, E., Benna, C., & Somov, B. V. 1996, *ApJ*, 456, 833
- Berghöfer, T. W., & Schmitt, J. H. M. M. 1994, *A&A*, 290, 435
- Berghöfer, T. W., Schmitt, J. H. M. M., Danner, R., & Cassinelli, J. P. 1997, *A&A*, 322, 167
- Brown, J. C., Dwivedi, B. N., Almeaky, Y. M., & Sweet, P. A. 1991, *A&A*, 249, 283
- Blumenthal, G. R., Drake, G. W. F., & Tucker, W. H. 1972, *ApJ*, 172, 205
- Cassinelli, J. P., & MacGregor, K. B. 1999, in *IAU Colloq. 175, The Be Phenomenon in Early Type Stars*, eds., M. Smith, H. Henrichs & F. Fabregat (San Francisco, ASP), p. 337
- Cassinelli, J. P., & Olson, G. L. 1979, *ApJ*, 229, 403
- Cassinelli, J. P., & Swank, J. H. 1983, *ApJ*, 271, 681
- Feldmeier, A. 1995, *A&A*, 299, 523
- Feldmeier, A., Puls, J., & Pualdrach, A. W. A. 1997, *A&A*, 322, 878
- Gabriel, A. H., & Jordan, C. 1969, *MNRAS*, 145, 241
- Keenan, F. P., 1994, McKenzie, D. L., Phillips, K. J. H., & Conlon, E. S. 1994, *ApJ*, 426, 454
- Kurucz, R. L. 1993, in *ASP Conf. Series, Peculiar Versus Normal Phenomena in A-Type and Related Stars*, eds., M. M. Dworetzky, F. Castelli, & R. Faraggiana, Vol. 44, p. 87
- Henrichs, H. F., et al. 2000, *A&A*, preprint
- Lamers, H. J. G. L. M., & Leitherer, C. 1993, *ApJ*, 412, 771
- Lamers, H. J. G. L. M., & Morton, D. C. 1976, *ApJS*, 32, 715

- Lamers, H. J. G. L. M., Waters, L. B. F. M., & Wesselius, P. R. 1984, *ApJ*, 134, L17
- Lucy, L. B., & White, R. L. 1980, *ApJ*, 241, 300
- MacFarlane, J. J., Cassinelli, J. P., Welsh, B. Y., Vedder, P. W., Vallerger, J. V., & Waldron, W. L. 1991, *ApJ*, 380, 564
- MacFarlane, J. J., Cohen, D. H., & Wang, P. 1994, *ApJ*, 437, 351
- Marshall, H. 2000, Chandra Proposer's Observatory Guide, in press
- Moffat, A. F. J., & Robert, C. 1994, *ApJ*, 421, 310
- Owocki, S. P., Castor, J. I., & Rybicki, G. B. 1988, *ApJ*, 335, 914
- Phillips, K. J. H., Bhatia, A. K., Mason, H. E., & Zarro, D. M. 1996, *ApJ*, 466, 549
- Pradhan, A. K., & Shull, J. M. 1981, *ApJ*, 249, 821
- Vaiana, G. S., & Rosner, R. 1978, *Ann. Rev. Astron. Astrophys.*, 16, 393
- Waldron, W. L. 1984, *ApJ*, 282, 256
- Waldron, W. L., Corcoran, M. F., Drake, S. A., & Smale, A. P. 1998, *ApJS*, 118, 217
- Waldron, W. L., Corcoran, M. F., & Kitamoto, S. 1997, ASCA Cherry Blossom Workshop, Washington, D. C., April (unpublished)
- Wolfson, C. J., Doyle, J. G., Leibacher, J. W., & Phillips, K. J. H. 1983, *ApJ*, 269, 319